Progress in Natural Science: Materials International 26 (2016) 334–340

HOSTED BY

Contents lists available at ScienceDirect

Progress in Natural Science: Materials International

journal homepage: www.elsevier.com/locate/pnsmi

Original Research

Antifungal activity of magnetically separable Fe_3O_4/ZnO/AgBr nanocomposites prepared by a facile microwave-assisted method

Abolghasem Hoseinzadeh [a], Aziz Habibi-Yangjeh [a,*], Mahdi Davari [b]

[a] Department of Chemistry, Faculty of Science, University of Mohaghegh Ardabili, P.O. Box 179, Ardabil, Iran
[b] Department of Plant Protection, Faculty of Agriculture, University of Mohaghegh Ardabili, P.O. Box 179, Ardabil, Iran

ARTICLE INFO

Article history:
Received 25 December 2015
Received in revised form
17 June 2016
Accepted 20 June 2016
Available online 10 August 2016

Keywords:
Fe_3O_4/ZnO/AgBr
Antifungal activity
Magnetic nanocomposite
Fusarium
Microwave irradiation

ABSTRACT

In the present work, magnetically separable Fe_3O_4/ZnO/AgBr nanocomposites with different weight ratios of Fe_3O_4 to ZnO/AgBr were prepared by a facile microwave-assisted method. The resultant samples were characterized by X-ray diffraction (XRD), scanning electron microscopy (SEM), transmission electron microscopy (TEM), energy dispersive analysis of X-rays (EDX), and vibrating sample magnetometery (VSM). Antifungal activity of the as-prepared samples was evaluated against *Fusarium graminearum* and *Fusarium oxysporum* as two phytopathogenic fungi. Among the nanocomposites, the sample with 1:8 weight ratio of Fe_3O_4 to ZnO/AgBr was selected as the best nanocomposite. This nanocomposite inactivates *Fusarium graminearum* and *Fusarium oxysporum* at 120 and 60 min, respectively. Moreover, it was observed that the microwave irradiation time has considerable influence on the antifungal activity and the sample prepared by irradiation for 10 min showed the best activity. Moreover, the nanocomposite without any thermal treatment displayed the superior activity.

1. Introduction

It is well known that agricultural products are remarkably reduced due to the different plant diseases caused by various pathogens such as fungi. Hence, the management of fungal plant diseases is economically important [1]. Moreover, these diseases have considerable influence on quality of the crops due to secondary metabolites production such as mycotoxin by fungi that pose a serious threat to human and animal health. Up to now, different strategies have been applied to control these fungal diseases [2]. Chemical treatment of these pathogens is the main method used for plant protection. However, synthetic fungicides have different drawbacks such as toxicity to humans, instability, and fungicide resistance in fungi. It is clear that the controlling strategies should be safe for the human health and environment. Hence, the demands for effective controlling methods of fungal diseases have attracted significant attention from the research community [3–14]. On the other hand, the largest fresh water consumer is in agricultural field [15]. Due to scarcity of fresh water, properly treated wastewaters could be safely used for agricultural purposes. However, before using wastewaters, different pathogenic pollutants, especially fungi must be treated to decrease health risk of agricultural products. In recent years, different nanomaterials have been applied for inactivation of phytopathogenic fungi [8,11–14]. Among these materials, ZnO nanomaterials have fascinating properties such as low-cost, high chemical and physical stability, nontoxicity to animals, and compatibility with the environment without any harmful effect on the soil fertility [16–21]. However, there are generally two main drawbacks for efficiently application of ZnO nanomaterials as antifungals. Firstly, antifungal activity of pure ZnO nanomaterials is not high enough to satisfactorily use them in large-scale. Secondly, the recovery of the suspended nanosized ZnO from the large volumes of the inactivation systems using filtration and centrifugation are complicated, time-consuming, and expensive. Meanwhile, they cannot be entirely separated from the treated systems, leading to generation of secondary pollution. The first drawback could be tackled by using ZnO-based nanocomposites. To overcome the second drawback, magnetic materials can be applied for removing the nanosized materials by applying external magnetic field [22–26]. Therefore, preparing multifunctional nanocomposites based on ZnO with reasonable antifungal activity that can be cost-effectively recycled from the treated solution is of great importance. However, to the best of our knowledge, there is no report about microwave-assisted preparation and antifungal activity of magnetically separable Fe_3O_4/ZnO/AgBr nanocomposites.

* Corresponding author.
E-mail address: ahabibi@uma.ac.ir (A. Habibi-Yangjeh).
Peer review under responsibility of Chinese Materials Research Society.

http://dx.doi.org/10.1016/j.pnsc.2016.06.006

In these regards, we prepared Fe_3O_4/ZnO/AgBr nanocomposites with different weight ratios of Fe_3O_4 to ZnO/AgBr using a facile microwaved-assisted method and their antifungal activities were investigated against two plant pathogenic fungi including *Fusarium graminearum* and *Fusarium oxysporum* causal agents of wheat head blight and lentil-vascular wilt diseases, respectively. The microstructure, purity, morphology, and magnetic properties of the prepared samples were studied using X-ray diffraction (XRD), energy dispersive analysis of X-rays (EDX), scanning electron microscopy (SEM), transmission electron microscopy (TEM), and vibrating sample magnetometry (VSM). The results showed that the antifungal activity of the nanocomposites enhanced with increasing weight ratio of ZnO/AgBr to Fe_3O_4. Moreover, it was demonstrated that the concentration of the nanocomposite, microwave-irradiation time, and calcination temperature have considerable influence on the inactivation process.

2. Experimental

2.1. Materials

Zinc nitrate ($Zn(NO_3)_2 \cdot 4H_2O$), ferric chloride ($FeCl_3 \cdot 6H_2O$), ferrous chloride ($FeCl_2 \cdot 4H_2O$), silver nitrate, sodium bromide, ammonia, sodium hydroxide, absolute ethanol, and malt extract agar (MEA) were obtained from Merck and employed without further purification. Deionized water was used for the experiments. Fungal isolates which had identified using morphological and molecular methods, were prepared from Fungal Collection of University of Mohaghegh Ardabili (FCUMA) and was cultured on potato dextrose agar (PDA) for future use.

2.2. Instruments

The XRD patterns were recorded by a Philips Xpert X-ray diffractometer with Cu Kα radiation (λ=0.15406 nm), employing scanning rate of 0.04°/s in the 2θ range from 20° to 80°. Surface morphology and distribution of particles were studied by LEO 1430VP SEM, using an accelerating voltage of 15 kV. The purity and elemental analysis of the products were obtained by EDX on the same SEM instrument. For SEM and EDX experiments, the samples mounted on an aluminum support using a double adhesive tape coated with a thin layer of gold. The TEM investigations were performed by a Zeiss-EM10C instrument with an acceleration voltage of 80 kV. Magnetic properties of the samples were obtained using an alternating gradient force magnetometer (model AGFM, Iran). A domestic microwave oven (2.45 GHz and 1000 W) used for preparation of the samples. The pH of solutions was measured using a Metrohm digital pH meter of model 691.

2.3. Preparation of the samples

Nanoparticles of Fe_3O_4 were prepared by chemical co-precipitation method, and the detailed preparation procedure was described elsewhere [27]. Typically for preparation of Fe_3O_4/ZnO/AgBr nanocomposite with 8:1 weight ratio of ZnO/AgBr to Fe_3O_4, 0.064 g Fe_3O_4 nanoparticles were dispersed in 100 mL of water by bath sonicating for 30 min. Then, zinc nitrate tetrahydrate (1.305 g) and silver nitrate (0.263 g) were dissolved in the formed black suspension and mechanically stirred for 30 min. After that, aqueous solution of NaOH (5 M) was added dropwise into the suspension with stirring at room temperature until pH of the solution reached 10. After 30 min of stirring, aqueous solution of sodium bromide (0.319 g in 20 mL of water) was slowly added to the formed suspension. The suspension was irradiated in the microwave oven for 10 min with 55% of output. The formed brown suspension was centrifuged to get the precipitate out and washed two times with water and ethanol to remove the unreacted reagents and dried in an oven at 60 °C for 24 h. Other nanocomposites were also prepared by tuning the weight ratio and labeled as Fe_3O_4/ZnO/AgBr (1:2), Fe_3O_4/ZnO/AgBr (1:4), Fe_3O_4/ZnO/AgBr (1:6), Fe_3O_4/ZnO/AgBr (1:8), and Fe_3O_4/ZnO/AgBr (1:10).

2.4. Antifungal activity assay

The inactivation experiments in water were performed in a 200 mL cylindrical Pyrex reactor. The reactor was provided with water circulation arrangement to maintain the temperature at 25 °C. Fungal isolates were subcultured on synthetic nutrient-poor agar (SNA) and maintained at 25 °C for 7 days until spores developed. The spores were detached from the mycelia on SNA by washing the plates with sterile water. The suspension obtained was homogenized by mechanical agitation and the concentration was adjusted on 1×10^7 spores/mL using haemacytometer. The suspension was diluted in the bottle-reactors to obtain an initial spore concentration of 4×10^7 CFU/mL (CFU=colony forming unit). The nanocomposite was added to the suspension in different concentrations. Control samples were prepared by using a sterile water suspension of the test fungi spores. The fungal concentration during the inactivation process was measured using the plate counting technique. The plates were incubated for 15 h at 25 ± 2 °C in the dark before counting. The germinated and demolished spores were counted in treatments and control.

3. Results and discussion

Crystal structures of the Fe_3O_4/ZnO and Fe_3O_4/ZnO/AgBr nanocomposites with different weight ratios of Fe_3O_4 to ZnO/AgBr were characterized by XRD patterns, and the results are shown in Fig. 1. In the case of the Fe_3O_4/ZnO nanocomposite, the diffraction peaks are simply indexed to (100), (002), (101), (102), (110), (103), (200), (112), (201), (004), and (202) planes of wurtzite hexagonal crystalline ZnO (JCPDS file number of 65-3411) and face-centered cubic structure of Fe_3O_4 (JCPDS file number of 75-1610) [28,29]. Due to low intensity of the diffraction peaks for the Fe_3O_4 nanoparticles relative to the ZnO nanostructures and low weight ratio of Fe_3O_4 to ZnO, only (400) and (331) planes have observable intensity and some of the diffraction peaks of the Fe_3O_4 nanoparticles are not clearly seen. For the Fe_3O_4/ZnO/AgBr nanocomposites, the diffraction peaks ascribed to wurtzite hexagonal ZnO, cubic AgBr, and face-centered cubic Fe_3O_4 phases [28–30]. For the AgBr counterpart of the nanocomposite, (111), (200), (220),

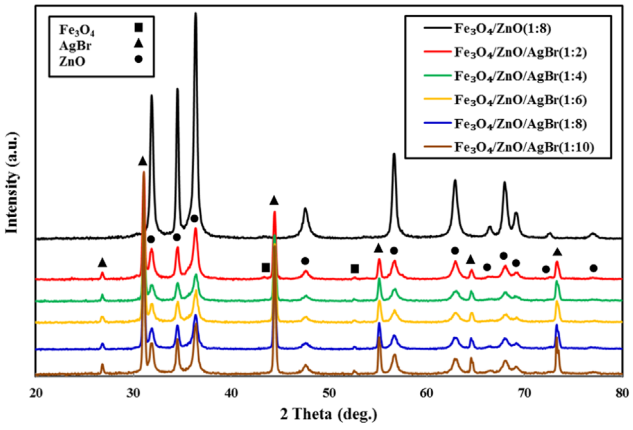

Fig. 1. XRD patterns of the Fe_3O_4/ZnO and Fe_3O_4/ZnO/AgBr nanocomposites with different weight ratios of Fe_3O_4 to ZnO/AgBr.

(222), (400), and (331) planes are clearly observed. Consequently, it was concluded that the Fe_3O_4/ZnO/AgBr nanocomposites were prepared by a fast microwave-assisted method and possible impurities such as $Zn(OH)_2$, Ag_2O, and AgOH did not form during the preparation procedure.

Purity of the samples was verified by EDX spectra and the results for the Fe_3O_4/ZnO and Fe_3O_4/ZnO/AgBr (1:8) samples are shown in Fig. 2(a). The peaks for Fe_3O_4/ZnO nanocomposite are obviously ascribed to Fe, O, and Zn elements. In the case of the Fe_3O_4/ZnO/AgBr (1:8) nanocomposite, the peaks are related to Fe, O, Zn, Ag, and Br elements. As can be seen, the samples have reasonable purity and all of the peaks are simply ascribed to the elements of the resultant nanocomposites. In addition, EDX mapping was applied to examine distributions of the elements in the Fe_3O_4/ZnO/AgBr (1:8) nanocomposite and the results are shown in Fig. 2(b)–(g). As can be seen, the elements of the nanocomposite have homogeneous distributions. Hence, it is concluded that in the nanocomposite Fe_3O_4, ZnO, and AgBr counterparts have uniformly combined to each other. Weight percents of Fe, O, Zn, Ag, and Br elements in this nanocomposite are 6.86, 18.31, 49.81, 14.52, and 10.50%, respectively.

Morphology of the Fe_3O_4/ZnO/AgBr (1:8) nanocomposite was investigated by SEM and TEM techniques and the results are shown in Fig. 3. As can be seen in SEM and TEM images, the particles of Fe_3O_4 and AgBr have distributed around the oval-like ZnO.

It is well known that the magnetic properties of materials can affect the magnetic separability of them [31]. Hence, the magnetization of the Fe_3O_4 nanoparticles and Fe_3O_4/ZnO/AgBr (1:8) nanocomposite were provided, and the results are shown in Fig. 4(a).

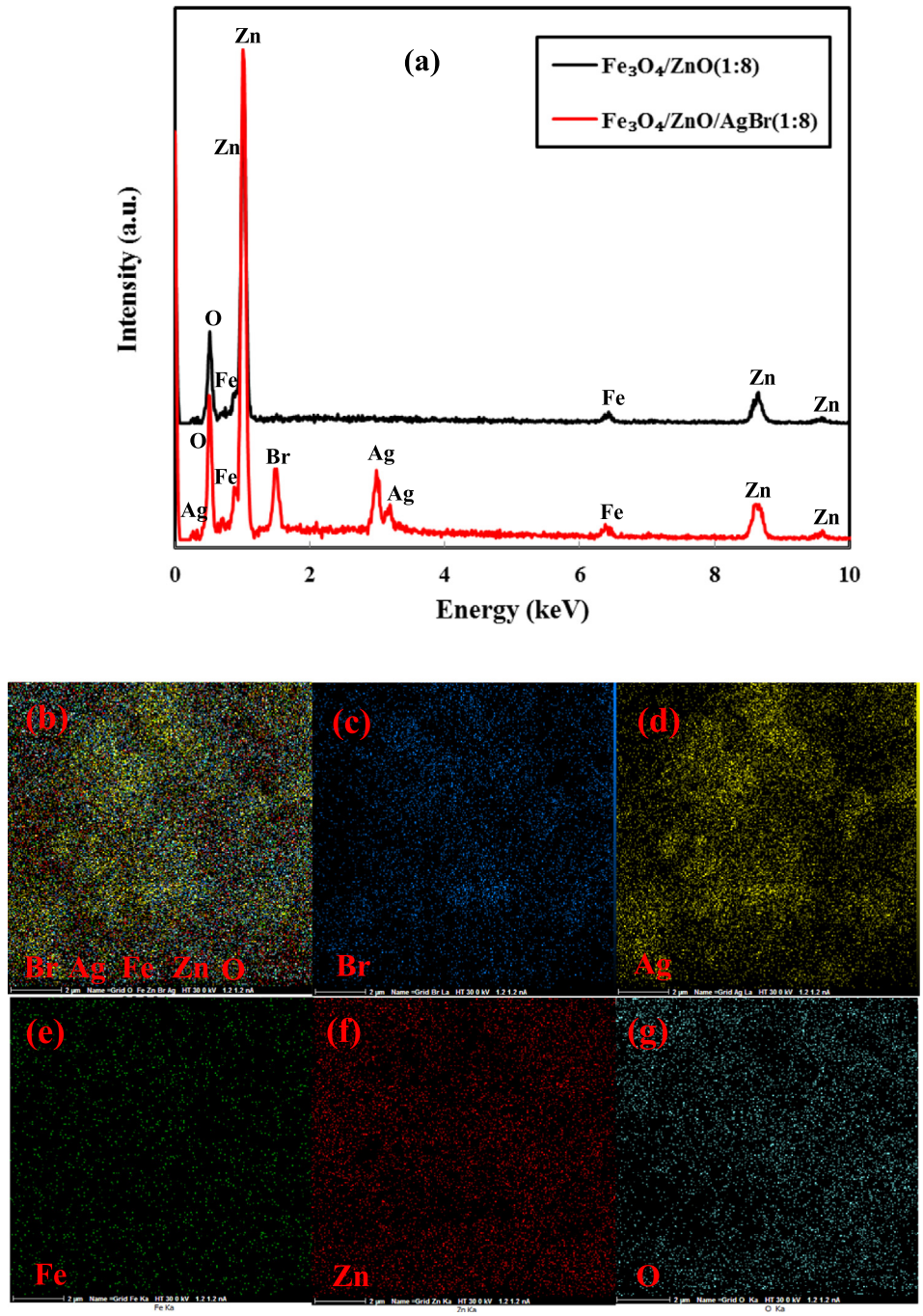

Fig. 2. (a) EDX spectra for the Fe_3O_4/ZnO and Fe_3O_4/ZnO/AgBr (1:8) nanocomposites. (b)-(g) EDX mapping of the Fe_3O_4/ZnO/AgBr (1:8) nanocomposite.

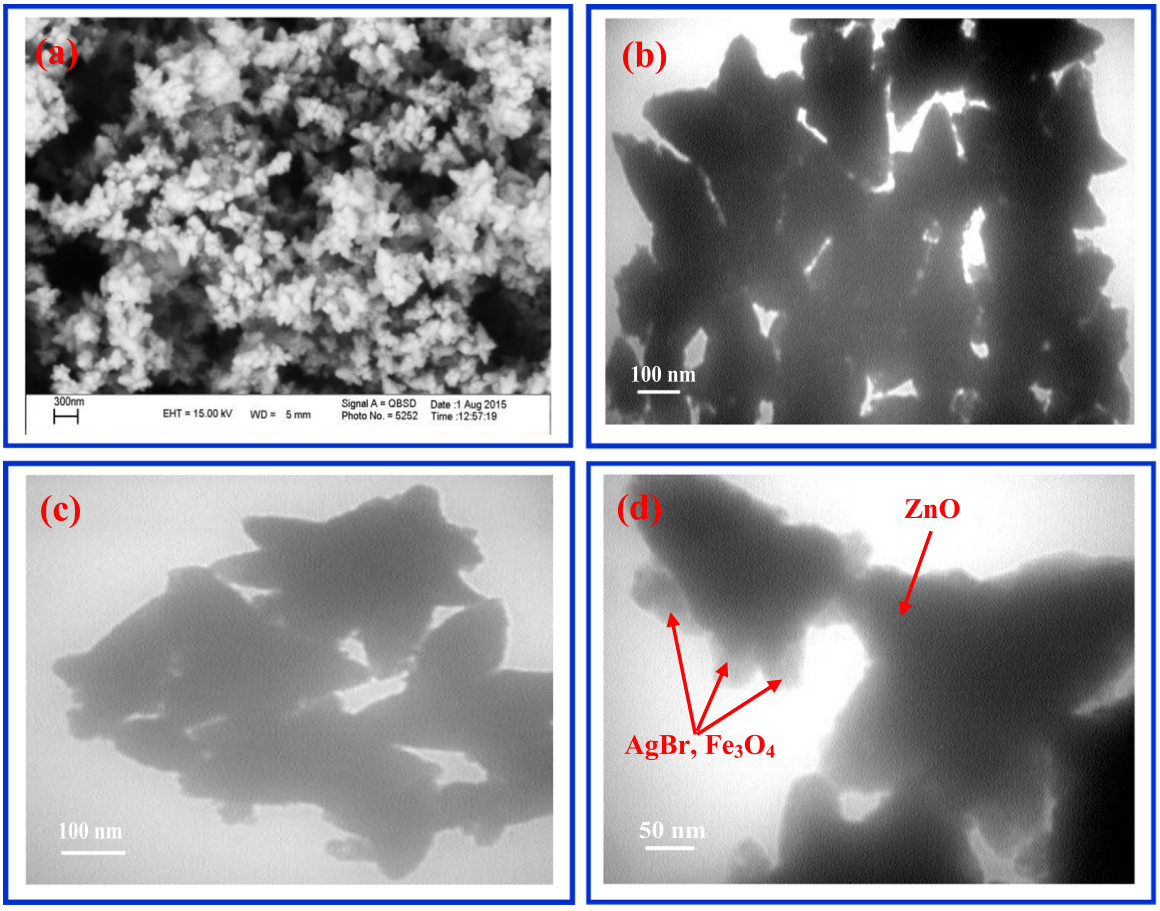

Fig. 3. (a) SEM and (b)-(d) TEM images of the Fe_3O_4/ZnO/AgBr (1:8) nanocomposite with different magnifications.

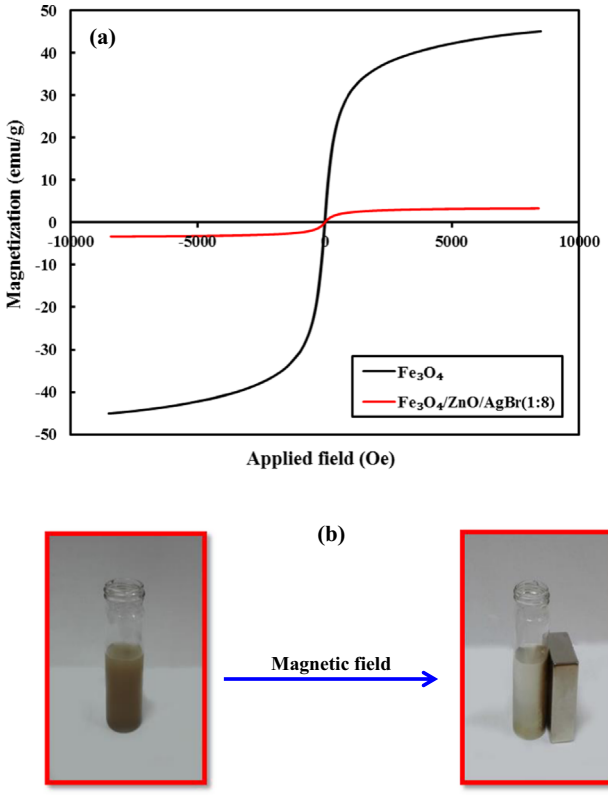

Fig. 4. (a) Magnetization curves for the Fe_3O_4 nanoparticles and Fe_3O_4/ZnO/AgBr (1:8) nanocomposite. (b) Magnetic separation of the Fe_3O_4/ZnO/AgBr (1:8) nanocomposite from the treated solution.

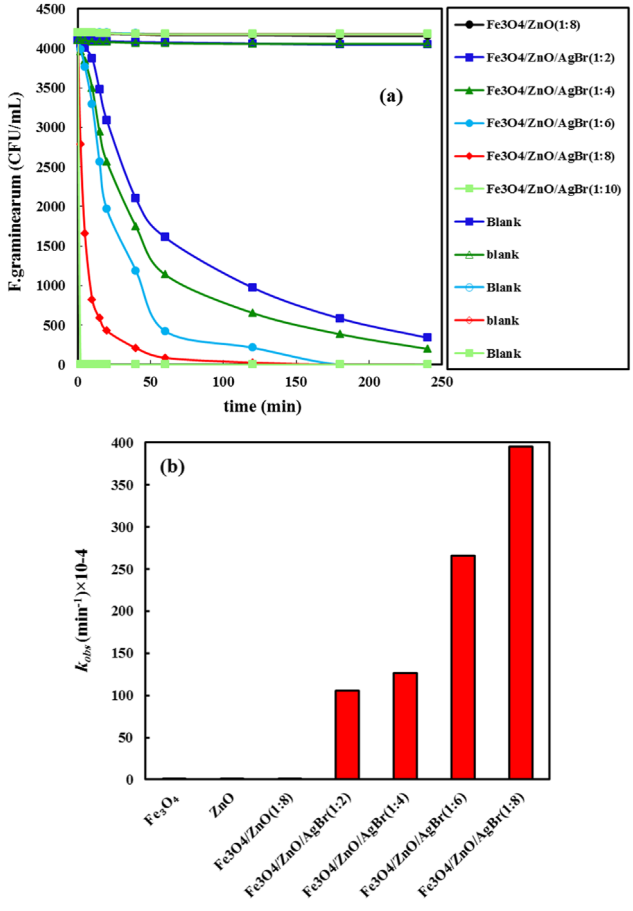

Fig. 5. (a) Inactivation of *Fusarium graminearum* over the nanocomposites with different weight ratios of Fe_3O_4 to ZnO/AgBr. (b) The inactivation rate constants over the different nanocomposites.

It is evident that the saturated magnetization for the Fe_3O_4 nanoparticles and the nanocomposite at 8500 Oe are 55.5 and 3.31 emu/g, respectively. Although the decrease of the magnetization for the nanocomposite is considerable, it is high enough to separate it from the solution after inactivation processes (Fig. 4 (b)). The decrease of the magnetization can be attributed to the presence of the nonmagnetic ZnO and AgBr along with the magnetic Fe_3O_4 nanoparticles [31].

Antifungal activity of the prepared samples was investigated against *Fusarium graminearum*, as an important plant pathogen. The inactivation process was performed over the Fe_3O_4/ZnO and Fe_3O_4/ZnO/AgBr nanocomposites with different weight ratio of Fe_3O_4 to ZnO/AgBr and the results are displayed in Fig. 5(a). Furthermore, parallel with the inactivation processes in presence of the nanocomposites, inactivations of the fungus in absence of any nanocomposite were carried out and the results are shown in this figure. It is evident that the fungus has reasonable stability in absence of the nanocomposites. Also, it is observed that the activities of the Fe_3O_4/ZnO/AgBr nanocomposites are higher than that of the Fe_3O_4/ZnO sample. Moreover, the antifungal activity of the nanocomposites increases with increasing weight ratio of ZnO/AgBr to Fe_3O_4. Among the prepared samples, the Fe_3O_4/ZnO/AgBr (1:10) nanocomposite displays the superior activity. It is evident that after 120 min, about 0.80, 76.2, 84.0, 94.8, and 99.4% of the fungus spores were inactivated over the Fe_3O_4/ZnO, Fe_3O_4/ZnO/AgBr (1:2), Fe_3O_4/ZnO/AgBr (1:4), Fe_3O_4/ZnO/AgBr (1:6), and Fe_3O_4/ZnO/AgBr (1:8) nanocomposites, respectively. Although antifungal activity of the Fe_3O_4/ZnO/AgBr (1:10) nanocomposite was higher than the other samples, due to its poor magnetic separability, the Fe_3O_4/ZnO/AgBr (1:8) nanocomposite was selected as the best sample.

In order to quantify antifungal activity of the resultant samples, first-order rate constants (k) of the inactivation processes over the nanocomposites were calculated using the slope of the following equation [32]:

$$\ln(N_t/N_o) = -kt \quad (1)$$

Where N_o and N_t represent the initial and at time of t fungus population (in cfu/mL), respectively. Moreover, k is the inactivation rate constant. As can be seen, the inactivation rate constant increases with weight ratio of ZnO/AgBr to Fe_3O_4 (Fig. 5(b)). The inactivation rate constants of the fungus over the Fe_3O_4/ZnO and Fe_3O_4/ZnO/AgBr (1:8) samples are 0.456×10^{-4} and 395×10^{-4} min^{-1}, respectively. Hence, activity of the Fe_3O_4@ZnO/AgBr (1:8) nanocomposite is about 866-folds larger than that of the Fe_3O_4/ZnO sample.

As seen in Fig. 6(a), *Fusarium graminearum* mocroconidia have degenerated over time. So that macroconidium germinated in control (a) while with a little germination after 20 min (b) and without germination after 60 min (c), and without germination and completely destruction at 120 min (d). In order to demonstrate the effect of the Fe_3O_4/ZnO/AgBr (1:8) nanocomposite on *Fusarium graminearum*, SEM images of that before (e) and after treatment (f) over the nanocomposite are shown in Fig. 6. As can be seen, in presence of the nanocomposite, the fungus has completely destroyed and damaged.

It is believed that in most cases inactivation of different microorganism over nanomaterials depends on concentration of them [32]. Hence, the investigation of the concentration effect is an important parameter from economical view point. To determine the effect of the nanocomposite concentration, a series of experiments were carried out by varying the nanocomposite concentration and the results are shown in Fig. 7(a). It is obvious

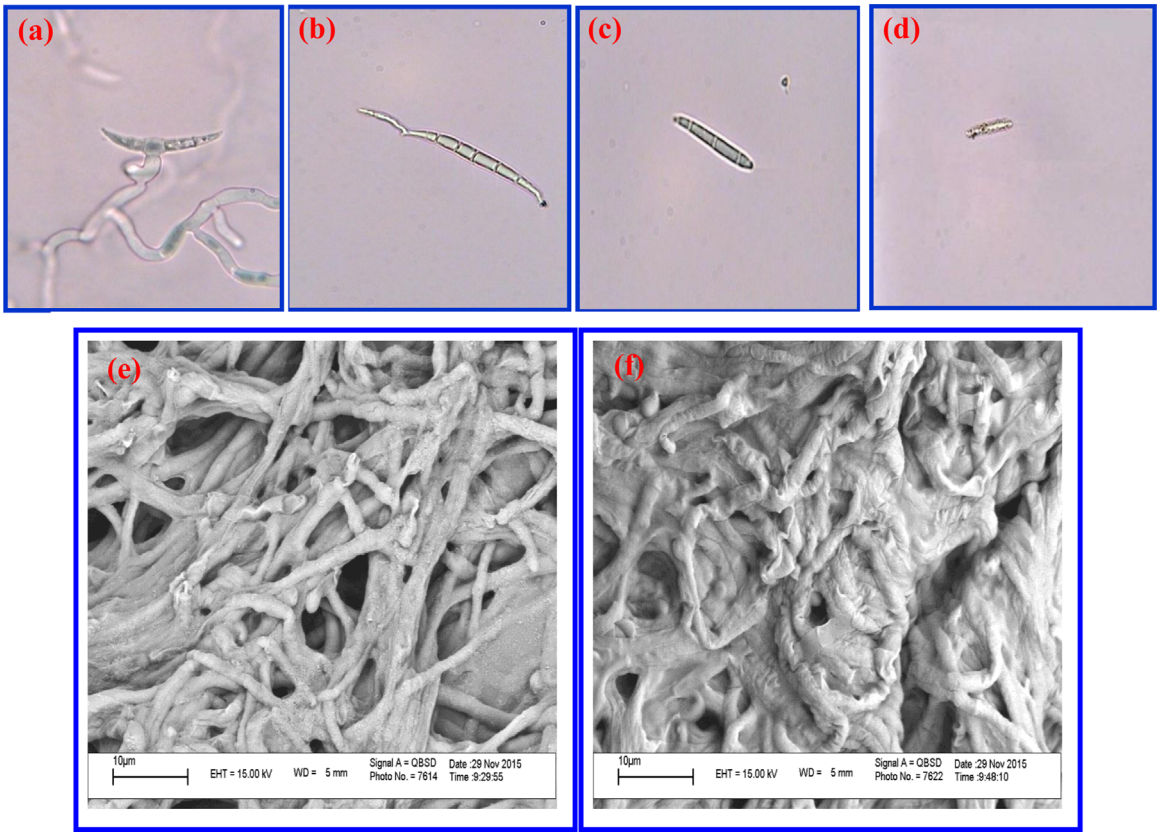

Fig. 6. Optical microscopic images for treatment of *Fusarium graminearum* by the Fe_3O_4/ZnO/AgBr (1:8) nanocomposite: (a) control, (b) after 20 min treatment, (c) after 60 min treatment, (d) after 120 min treatment. SEM images for inactivation of *Fusarium graminearum* over the Fe_3O_4/ZnO/AgBr (1:8) nanocomposite: (e) before inactivation and (f) after inactivation.

that the inactivation rate constant increases with concentration of the nanocomposite (Fig. 7(b)). This increase could be related to the presence of more nanocomposites adsorbed over the surface of the fungus.

It has been reported that the preparation time of nanocomposites can remarkably affect the morphology, crystallinity, aggregation, and size of the particles. Hence, the microwave-irradiation time could affect the antifungal activity of the prepared nanocomposites. To find the optimum preparation time, the Fe_3O_4/ZnO/AgBr (1:8) nanocomposite prepared by microwave irradiations for 2.5, 5, 10, 15, and 20 min, and the results are shown in Fig. 8(a). It is evident that the inactivation rate constant increases with increasing the preparation time up to 10 min and then decreases. Decrease of the antifungal activity of the samples prepared with higher microwave irradiation times could be related to more aggregation of the particles, resulting in decreased surface area of the nanocomposites [33].

It is well known that calcination of nanomaterials can change the crystallinity and size of the particles. To study the effect of calcination temperature on the antifungal activity, the Fe_3O_4/ZnO/AgBr (1:8) nanocomposite was calcined at 200, 400, and 600 °C for 2 h and the inactivation process was carried out over them and the results are shown in Fig. 8(b). It is clear that antifungal activity of the nanocomposite without any thermal treatment is higher than those of the other samples. The decrease of the antifungal activity at higher calcination temperatures could be attributed to growth of the particles at higher calcination temperatures [34,35].

It is well known that wastewaters contain mixtures of different fungi. Hence, the ability of an antifungal material to inactivate them as non-selectively is very important. To investigate the ability of the Fe_3O_4/ZnO/AgBr (1:8) nanocomposite for inactivation

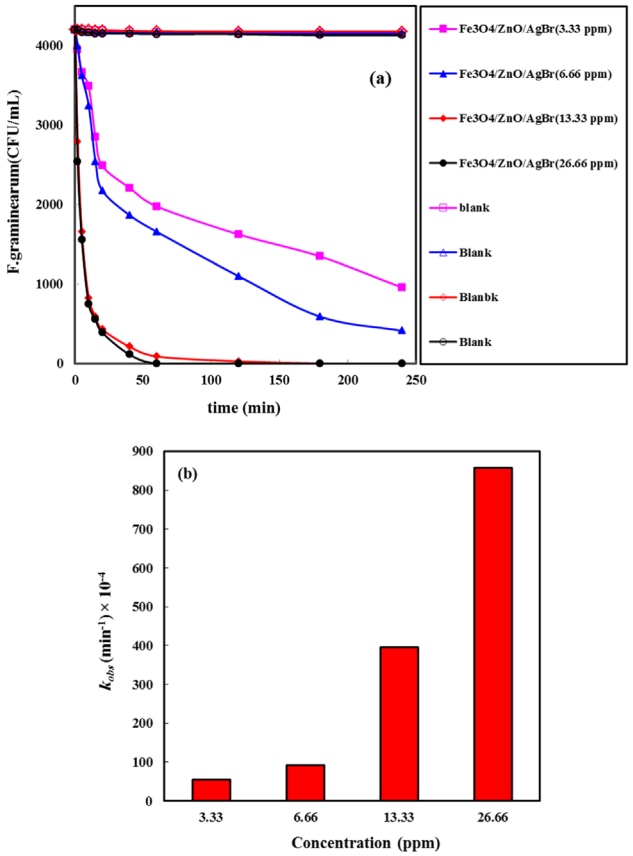

Fig. 7. (a) Inactivation of *Fusarium graminearum* over the Fe_3O_4/ZnO/AgBr (1:8) nanocomposite with different concentrations. (b) The inactivation rate constants over the nanocomposite with different concentrations.

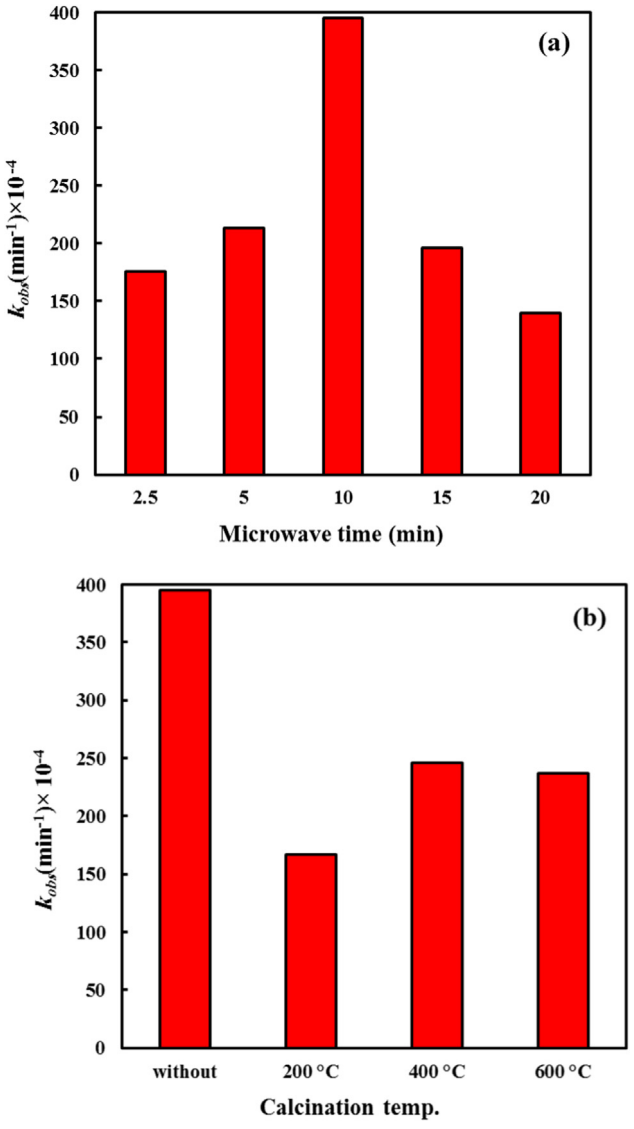

Fig. 8. (a) The inactivation rate constants of *Fusarium graminearum* over the Fe_3O_4/ZnO/AgBr (1:8) nanocomposite prepared at different microwave-irradiation times. (b) The inactivation rate constants of *Fusarium graminearum* over the Fe_3O_4/ZnO/AgBr (1:8) nanocomposite calcined at different temperatures.

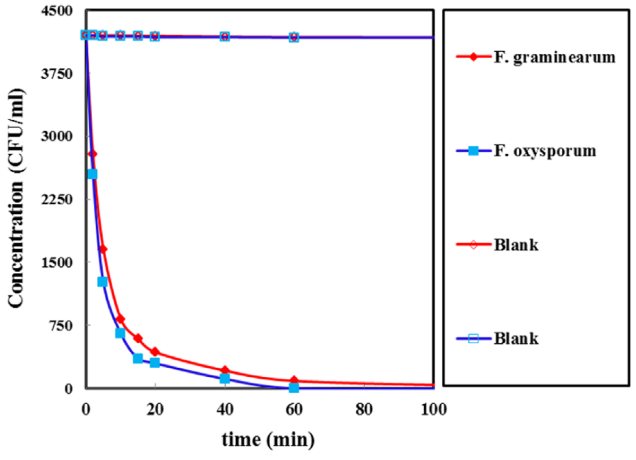

Fig. 9. Comparison between inactivation of *Fusarium graminearum* and *Fusarium oxysporum* over the Fe_3O_4/ZnO/AgBr (1:8) nanocomposite.

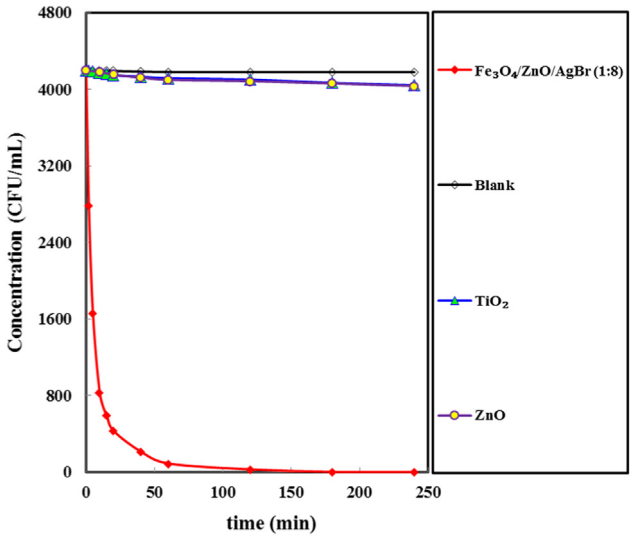

Fig. 10. Comparison between antifungal activity of the Fe_3O_4/ZnO/AgBr (1:8) nanocomposite with the ZnO and TiO_2 (P25).

of another fungus, inactivation of *Fusarium oxysporum* was studied, and the results were compared with *Fusarium graminearum* (Fig. 9). As can be seen, the nanocomposite completely inactivated *Fusarium oxysporum* in 60 min, which is some smaller than that of *Fusarium graminearum*. Hence, it is confirmed that the magnetic Fe_3O_4/ZnO/AgBr (1:8) nanocomposite has considerable activity in inactivation of two different fungi. Moreover, in order to show enhanced antifungal activity of this nanocomposite, Fig. 10 displays comparison between antifungal activities of the Fe_3O_4/ZnO/AgBr (1:8) nanocomposite with ZnO and TiO_2 (P25) against *Fusarium graminearum*. It is clear that the nanocomposite has excellent activity relative to the ZnO and TiO_2. Therefore, this nanocomposite has not only great antifungal activity but also considerable magnetic recyclability, which are important in wastewater treatments. Finally, to confirm stability of the nanocomposite, the nanocomposite was recovered and dried after the inactivation process and its composition was analyzed using EDX mapping. Wight percents of Fe, O, Zn, Ag, and Br elements were 5.83%, 19.34%, 50.84%, 12.49%, and 11.50%, respectively, which are close to the composition of the nanocomposite before using (6.86%, 18.31%, 49.81%, 14.52%, and 10.50%).

4. Conclusions

The multifunctional Fe_3O_4/ZnO/AgBr nanocomposites were prepared by a cost-effective microwave-assisted method. The resultant samples were characterized by XRD, SEM, TEM, EDX, and VSM techniques. Among the prepared samples, the Fe_3O_4/ZnO/AgBr (1:8) nanocomposite has the best antifungal activity toward *Fusarium graminearum*, as a phytopathogenic fungus. This nanocomposite completely inactivated *Fusarium oxysporum* in 60 min, which is some smaller than the time for *Fusarium graminearum*. The inactivation rate constant increases with the concentration of the nanocomposite. Moreover, the antifungal activity of the nanocomposite prepared by 10 min microwave irradiation is superior to those of the other preparation times. These results suggest that the prepared magnetic nanocomposites could be used as an effective fungicide in agricultural and wastewater treatments. More importantly, the nanocomposite can be recycled from the place of action by means of an external magnetic field.

References

[1] L. Gilchrist, H.J. Dubin, Fusarium head blight, in: B.C. Curtis, S. Rajaram, H. Go´mez Macpherson (Eds.), FAO Plant Production and Protection Series No. 30, Food and Agriculture Organization of the United Nations, Rome, 2002.
[2] M.I. Polo-López, M. Castro-Alférez, I. Oller, P. Fernández-Ibáñez, Chem. Eng. J. 257 (2014) 122–130.
[3] P. Fernández-Ibáñez, C. Sichel, M.I. Polo-López, M. de Cara-García, J.C. Tello, Catal. Today 144 (2009) 62–68.
[4] S. Fateixa, M.C. Neves, A. Almeida, J. Oliveira, T. Trindade, Colloids Surf. B: Biointerfaces 74 (2009) 304–308.
[5] M.I. Polo-López, P. Fernández-Ibáñez, I. García-Fernández, I. Oller, I. SalgadoTránsito, C. Sichel, J. Chem. Technol. Biotechnol. 85 (2010) 1038–1048.
[6] B. Chudasama, A.K. Vala, N. Andhariy, R.V. Upadhyay, R.V. Mehta, J. Magn. Magn. Mater. 323 (2011) 1233–1237.
[7] M.I. Polo-López, I. García-Fernández, I. Oller, P. Fernández-Ibáñez, Photochem. Photobiol. Sci. 10 (2011) 381–388.
[8] S.W. Kim, J.H. Jung, K. Lamsal, Y.S. Kim, J.S. Min, Y.S. Lee, Mycobiology 40 (2012) 53–58.
[9] P. Patra, S. Mitra, N. Debnath, A. Goswami, Langmuir 28 (2012) 16966–16978.
[10] A. Turki, H. Kochkar, I. Garcia-Fernandez, M.I. Polo-Lopez, A. Ghorbel, C. Guillard, G. Berhault, P. Fernadez-Ibanez, Catal. Today 209 (2013) 147–152.
[11] K.-P. Yu, Y.-T. Huang, S.-C. Yang, J. Hazard. Mater. 261 (2013) 155–162.
[12] K. Phiwdang, M. Phensaijai, W. Pecharapa, Adv. Mater. Res. 802 (2013) 89–93.
[13] T.R. Lakshmeesha, M.K. Sateesh, B.D. Prasad, S.C. Sharma, D. Kavyashree, M. Chandrasekhar, H. Nagabhushana, Cryst. Growth Des. 14 (2014) 4068–4079.
[14] X. Wang, X. Liu, J. Chen, H. Han, Z. Yuan, Carbon 68 (2014) 798–806.
[15] F.A.O. Statistical, Yearbook, FAO Electronic Publishing, Food and Agriculture Organization of the United Nations, Rome, 2006.
[16] M. Eskandari, N. Haghighi, V. Ahmadi, F. Haghighi, S.H.R. Mohammadi, Physica B 406 (2011) 112–114.
[17] L. He, Y. Liu, A. Mustapha, M. Lin, Microbiol. Res. 166 (2011) 207–215.
[18] M.A. Gondal, A.J. Alzahrani, M.A. Randhawa, M.N. Siddiqui, J. Environ. Sci. Health, Part A 47 (2012) 1413–1418.
[19] C.O. Dimkpa, J.E. McLean, D.W. Britt, A.J. Anderson, Biometals 26 (2013) 913–924.
[20] R.K. Sharma, R. Ghose, Ceram. Int. 41 (2015) 967–975.
[21] N. Sharma, S. Jandaik, S. Kumar, M. Chitkara, I.S. Sandhu, J. Exper., Nanosci (2015) http://dx.doi.org/10.1080/17458080.2015.1025302.
[22] R. Prucek, J. Tucek, M. Kilianová, A. Panácek, L. Kvítek, J. Filip, M. Kolár, K. Tománková, R. Zboril, Biomaterials 32 (2011) 4704–4713.
[23] S. Singh, K.C. Barick, D. Bahadur, J. Mater. Chem. A 1 (2013) 3325.
[24] Z. Markova, K.M. Siskova, J. Filip, J. Cuda, M. Kolar, K. Safarova, I. Medrik, R. Zboril, Environ. Sci. Technol. 47 (2013) 5285–5293.
[25] S. Zhan, Y. Yang, Z. Shen, J. Shan, Y. Li, S. Yang, D. Zhu, J. Hazard. Mater. 274 (2014) 115–123.
[26] S. Zhan, D. Zhu, S. Ma, W. Yu, Y. Jia, Y. Li, H. Yu, Z. Shen, ACS Appl. Mater. Interf. 7 (2015) 4290–4298.
[27] R. Massart, Magn. IEEE Trans 17 (1981) 1247–1248.
[28] B.G. Mishra, G.R. Rao, J. Mol. Catal. A: Chem 243 (2006) 204–213.
[29] J. Safari, Z. Zarnegar, J. Mol. Struct. 1072 (2014) 53–60.
[30] M. Pirhashemi, A. Habibi-Yangjeh, Appl. Surf. Sci. 283 (2013) 1080–1088.
[31] W. Wu, C. Jiang, V.A.L. Roy, Nanoscale 7 (2015) 38–58.
[32] O.K. Dalrymple, E. Stefanakos, M.A. Trotz, D.Y. Goswami, Appl. Catal. B: Environ 98 (2010) 27–38.
[33] M. Shekofteh-Gohari, A. Habibi-Yangjeh, Ceram. Int. 41 (2015) 1467–1476.
[34] S.Y. Kim, T.H. Lim, T.S. Chang, C.H. Shin, Catal. Lett. 117 (2007) 112–118.
[35] A. Singh, D.P. Dutta, A. Ballal, A.K. Tyagi, M.H. Fulekar, Mater. Res. Bull. 51 (2014) 447–454.